



## COMPARISONS BETWEEN CONSTANT, LINEAR, QUADRATIC, SPLINE AND SINGULAR ELEMENTS IN THE 2D DYNAMIC SOIL-STRUCTURE INTERACTION BEM ANALYSIS.

**Pérsio Leister de Almeida Barros**

Faculdade de Engenharia Civil, Universidade Estadual de Campinas  
Caixa Postal 6021, CEP 13083-970, Campinas, SP.

**Euclides de Mesquita Neto**

Faculdade de Engenharia Mecânica, Universidade Estadual de Campinas  
Caixa Postal 6122, CEP 13083-970, Campinas, SP.

**Abstract.** *The article presents the determination of the dynamic response of a rigid strip footing bonded to a viscoelastic half-space using an indirect BEM formulation with various interface traction interpolation models. Non singular constant linear, quadratic and spline interpolation models and singular linear and spline interpolation models are used. Resulting interface traction distribution and rotation of the foundation subjected to a rocking moment are presented and analyzed. The numeric results show that the singular models provide much smoother traction distribution and better convergence for the foundation rotation.*

**Keywords:** *Elastodynamics, Boundary Element Method, Soil-structure interaction, Singular functions, Splines.*

### 1. INTRODUCTION

The dynamic response of a rigid foundation resting over or embedded in an elastic medium has been obtained, in general, by the Boundary Element Method. Additionally, it is a common practice to use half-space Green's and influence functions in such analyses. This makes the discretization necessary only at the soil-structure interface. After the discretization, normally a constant stress distribution is adopted along each formed element. This methodology was first employed by Lysmer (1965) in the analysis of a rigid disk over a half-space, loaded vertically. In the case of plane strain problems, such as the analysis of rigid strip-footings, the use of constant-stress elements provides reasonable results for the vertical and horizontal displacements of the foundation using only a moderate number of elements. For the foundation rotation, however, the convergence of the results is much slower. Even more, the interface stresses obtained show an unsatisfactory distribution, with sudden signal inversions and many oscillations, particularly near the foundation edges. This behavior is also observed for the vertical and horizontal dynamic loads. As a consequence, there is little confidence on the quality of the obtained displacements.

In order to remove this uncertainty and to obtain a better estimation of the displacements

and interface stress distributions an extensive study was conducted. The main purpose of this study was to develop BEM solutions for the strip-foundation problem using stress distribution models other than the standard constant stress distribution and to analyze the results of both displacements and interface stresses obtained with each model.

The first step was to try to use polynomial interpolation models of higher order. Linear and quadratic distribution along each interface element were used. As a second step, spline functions were used to interpolate the stresses along the soil-foundation interface. Finally, singular stress interpolation elements were used at the foundation edges.

This article describes all these models and the general formulation of them. Comparisons are made for the results obtained with each model, in terms of interface stresses and displacements.

## 2. STATEMENT OF THE PROBLEM AND GENERAL SOLUTION

The problem to be used in the analysis is illustrated in Figure 1. It represents a rigid massless strip footing resting on (and bonded to) the surface of a viscoelastic half-space and subjected to a set of dynamic external forces and moment. These forces and the moment are applied harmonically in time with frequency  $\omega$ , so the analysis can be performed in frequency domain. The footing is infinitely long in  $y$  direction and the loading is uniformly distributed along the  $y$  axis, so it can be considered a plane-strain problem. The objective is to determine the steady state response of the footing under the influence of the external forces.

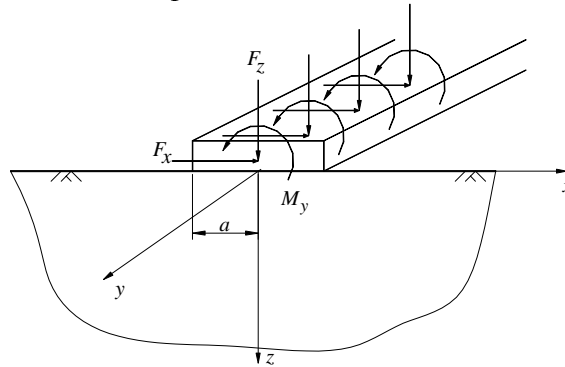


**Figure 1:** Rigid strip footing bonded to a viscoelastic half-space

The response of the rigid structure can be expressed by the equation:

$$\begin{Bmatrix} w_0 \\ u_0 \\ a\phi_0 \end{Bmatrix} = \frac{1}{G} \begin{bmatrix} N_{wz} & 0 & 0 \\ 0 & N_{ux} & N_{um} \\ 0 & N_{\phi x} & N_{\phi m} \end{bmatrix} \begin{Bmatrix} F_z \\ F_x \\ M_y/a \end{Bmatrix} \quad (1)$$

where  $w_0$ ,  $u_0$  and  $\phi_0$  are the (complex) vertical, horizontal displacements and rotation of the footing, respectively, and  $G$  is the shear modulus of the elastic medium. The displacements and rotation are related to the applied (complex) external forces by the compliance matrix, the elements of which,  $N_{ij}$ , are complex and, in general, frequency dependent.

The compliance matrix is obtained by the *superposition method*, a specialized version of the indirect formulation of the BEM that uses half-space solutions (Barros, 1997). Within the superposition method, first the soil-structure interface is discretized with  $N$  elements and an interpolation model for the tractions  $t_x$  and  $t_z$  along this interface is chosen. These tractions

should satisfy the equilibrium conditions:

$$F_z = \int_{-a}^a t_z(x) dx, \quad F_x = \int_{-a}^a t_x(x) dx, \quad M_y = - \int_{-a}^a x t_z(x) dx \quad (2)$$

As there are  $N$  elements, these equilibrium equations can be expressed as a summation and written in a matrix equation with the general form:

$$\{\mathbf{f}\} = [\mathbf{D}] \{\mathbf{t}\} \quad (3)$$

Additionally, the displacements  $u$  and  $w$  along the interface should satisfy the rigid body motion conditions. If the chosen interpolation model has  $N^*$  degrees of freedom, it will be necessary to apply these conditions to  $N^*$  nodes. The set of equations can be written as:

$$\{\mathbf{u}\} = [\mathbf{C}] \{\mathbf{u}_0\} \quad (4)$$

On the other hand, the displacements of the points at the interface are functions of the interface tractions and can be determined by the superposition of *influence functions* with the general form (Rajapakse and Wang, 1991):

$$u_{ij}(x) = \frac{1}{\sqrt{2\pi}} \int_{-\infty}^{\infty} \bar{t}(\lambda) \bar{U}_{ij}(\omega, \lambda) e^{i\lambda x} d\lambda, \quad i = x, z \quad (5)$$

where  $u_{ij}$  is the displacement in the  $i$ -th direction caused by a surface traction acting in the  $j$ -th direction. Also,  $\lambda$  is the wave number,  $\bar{U}_{ij}$  is the Fourier-transform of the displacement general solution for a concentrated line load applied on the surface of an elastic half-space (or another soil profile with a known solution) and  $\bar{t}$  is the Fourier-transform of the traction distribution function. The superposition of the traction-displacement relation (5) for the  $N^*$  nodes leads to the following system of equations:

$$\{\mathbf{u}\} = [\mathbf{U}] \{\mathbf{t}\} \quad (6)$$

The final system of equations has the general form:

$$\begin{bmatrix} \mathbf{U} & -\mathbf{C} \\ \mathbf{D} & \mathbf{0} \end{bmatrix} \begin{Bmatrix} \mathbf{t} \\ \mathbf{u}_0 \end{Bmatrix} = \begin{Bmatrix} \mathbf{0} \\ \mathbf{f} \end{Bmatrix} \quad (7)$$

To obtain the elements  $N_{ij}$  of the compliance matrix, one can set individually each element of  $\mathbf{f}$  to one and solve the system of equations given by (7).

### 3. CONSTANT INTERPOLATION MODEL

The simplest form of interpolation for the interface tractions is the constant interpolation model. The tractions are assumed to be constant along each interface element, as can be seen in the Figure 2(a).

For this model the number of degrees of freedom  $N^*$  equals the number of elements  $N$ , so there are  $N$  nodal points located at the center point of each element. At these nodal points the rigid body motion conditions, as expressed by equations (4), are imposed. For this calculation an unitary constant traction strip distribution (see Figure 2(b)) is used.

The constant-type traction distribution  $t^{(0)}(x)$  is defined as:

$$t^{(0)}(x) = \begin{cases} 1 & \text{if } -l \leq x \leq l \\ 0 & \text{otherwise} \end{cases} \quad (8)$$

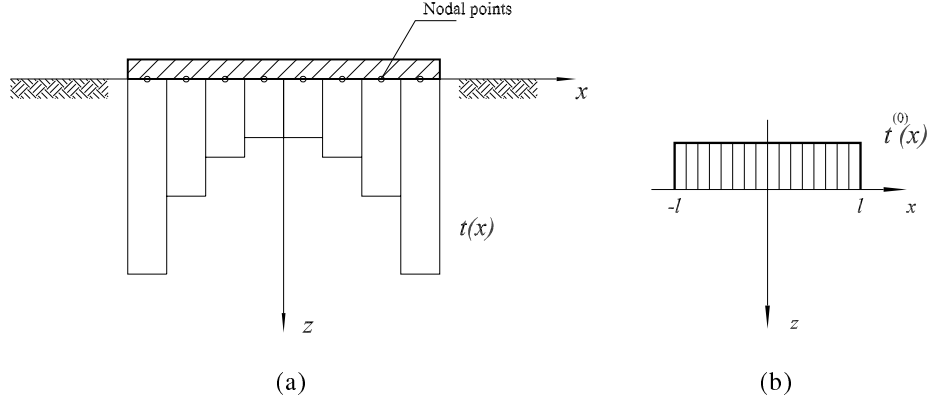


**Figure 2:** (a) Constant interpolation model for the interface tractions  $t_x$  and  $t_z$ , (b) Constant-type tractions distribution

where  $l$  is the half-width of the strip.

The influence functions (5) for the constant model are calculated for the constant traction at each one of the  $N$  elements and for the  $N$  nodal points. So this evaluation has to be performed  $N \times N$  times. This is by far the more lengthy operation of the whole analysis because of the numerical integration involved in the influence function calculation. As a consequence, it is important to keep the number of influence function evaluation as low as possible, from the computational efficiency point of view. This can be accomplished by making all the elements the same length. By using this strategy only one line of the influence matrix  $\mathbf{U}$  must be evaluated and the other lines of  $\mathbf{U}$  can be obtained from this first line. The number of influence function evaluation is then reduced to  $N$ . The Table 1 shows the number of influence function evaluations for this and the other interpolation models used in this work.

The Figure 3 shows the interface traction distribution  $t^* = a^2 t / M_y$  that results from the analysis of a rigid strip footing subjected to an external applied dynamic moment  $M_y$  using 16 constant-type traction elements. The Poisson ratio of the medium is  $\nu = 0.4$  and the material internal damping factor is  $\nu = 0.01$ . For this analysis it was used a non-dimensional frequency  $a_0 = a\omega / c_s = 1.0$ , where  $c_s$  is the shear wave velocity in the elastic medium.

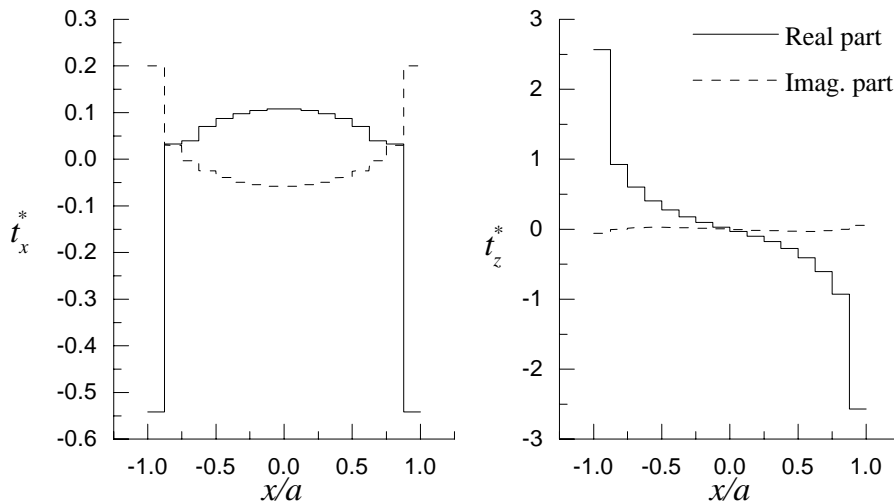


**Figure 3:** Interface traction  $t^*(x)$  distribution for an applied moment  $M_y$  ( $a_0 = 1, \nu = 0.4$ ).

The results for the interface stresses in Figure 3 show that there are very high differences between the stress values for consecutive elements near the foundation edges. This suggests

that the use of higher degree interpolation models could improve the analysis.

#### 4. LINEAR AND QUADRATIC INTERPOLATION MODELS

The linear and quadratic interpolation models are natural steps following the constant model. In these models the interface stresses are assumed to take a linear and quadratic polynomial variation within each interface element (see Figures 4(a) and 4(b)).

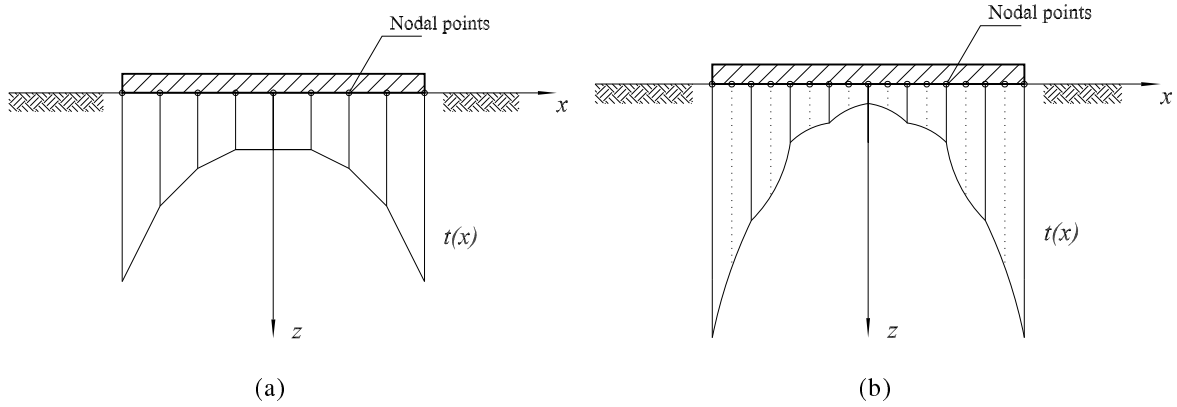


**Figure 4:** (a)Linear and (b)quadratic interpolation models for the interface tractions  $t_x$  and  $t_z$

The influence functions involved in the determination of the nodal points displacements are obtained by the superposition of (properly weighted) unitary constant, linear and quadratic strip traction distributions. The linear and quadratic distributions are defined as:

$$t^{(k)}(x) = \left(\frac{x}{l}\right)^k, \quad k = 1, 2, \quad |x| \leq l \quad (9)$$

The plots in Figures 5 and 6 show  $t_x^*$  and  $t_z^*$  distributions for an applied dynamic moment  $M_y$ . For the linear interpolation model the interface was discretized in 16 elements and for the quadratic model it was used 8 elements.

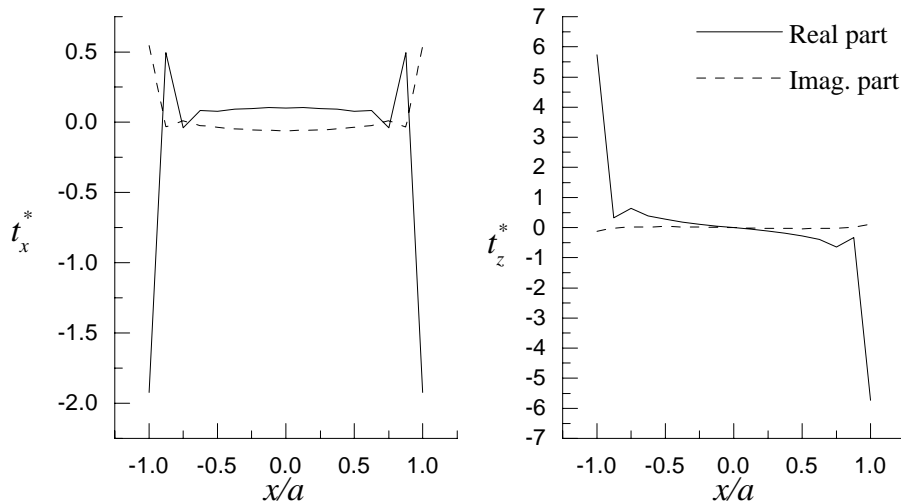


**Figure 5:** Interface traction  $t^*(x)$  distribution due to an applied moment  $M_y$  (linear model,  $a_0 = 1$ ,  $\nu = 0.4$ ).

As can be seen in Figures 5 and 6, the linear and quadratic element models lead to non-smooth stress distributions. These distributions present strong oscillations near the foundation

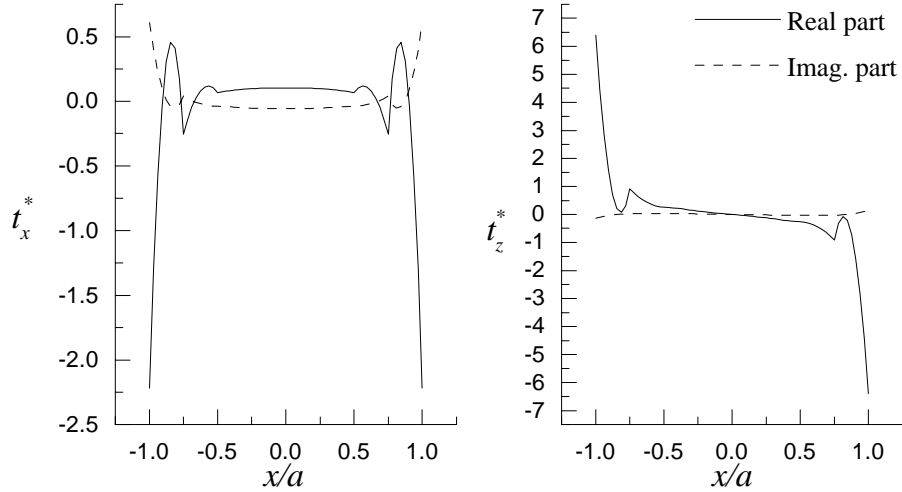


**Figure 6:** Interface traction  $t^*(x)$  distribution due to an applied moment  $M_y$  (quadratic model,  $a_0 = 1$ ,  $\nu = 0.4$ ).

edges. The oscillations become even more pronounced as the degree of the interpolation model is increased. It is evident that the interface stresses present a singular behavior at the foundation edges. The polynomial interpolation incapacity to correctly model this singularity seems to contaminate the solution throughout the whole interface.

## 5. SPLINE INTERPOLATION MODELS

Another traction interpolation model that can be applied to the problem analysis is the spline model. Within this model the interface tractions are assumed to have higher order continuity throughout the interface. Two spline types were used in the present analysis. The first one is the Overhauser spline (Brewer and Anderson, 1977) that provides  $C^1$  continuity. The other is the cubic spline (de Boor, 1978) that provides  $C^2$  continuity. These two splines use cubic polynomial segments along each element, so one more type of influence function ( $t^{(3)}$ ) is required. The definition of this strip traction distribution follows from equations (9).

The cubic polynomial segments that make up the splines are defined as (see Figure 7) (Barros and Mesquita Neto, 1999):

$$t(x) = \sum_{k=0}^3 c_{ik} \left( \frac{x - \bar{x}_i}{l_i} \right)^k, \quad x_i \leq x \leq x_{i+1}, \quad i = 1, \dots, N \quad (10)$$

with

$$\bar{x}_i = \frac{x_{i+1} + x_i}{2}, \quad l_i = \bar{x}_i - x_i \quad (11)$$

The parameters  $c_{ik}$  of the polynomials are given by:

$$\begin{aligned} c_{i0} &= \frac{1}{2}(t_i + t_{i+1}) + \frac{l_i}{4}(s_i - s_{i+1}) & c_{i1} &= -\frac{3}{4}(t_i - t_{i+1}) - \frac{l_i}{4}(s_i + s_{i+1}) \\ c_{i2} &= -\frac{l_i}{4}(s_i - s_{i+1}) & c_{i3} &= \frac{1}{4}(t_i - t_{i+1}) + \frac{l_i}{4}(s_i + s_{i+1}), \quad i = 1, \dots, N \end{aligned} \quad (12)$$

where  $s_i = t'(x_i)$ . For the cubic spline, the value of  $s_i$  is obtained imposing continuity of the second derivative at the internal data points  $x_i, i = 2, \dots, N$  plus two additional end conditions

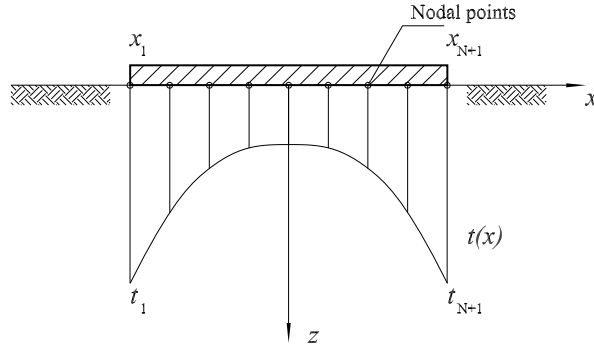


**Figure 7:** Spline traction distribution model

given by  $t''(x_1) = t''(x_{N+1}) = 0$ . In the case of the Overhauser spline, each  $s_i$  is obtained by setting a parabola through  $t_{i-1}$ ,  $t_i$  and  $t_{i+1}$ , and taking the derivative of this parabola at  $x_i$ .

The plots in Figure 8 show  $t_x^*$  and  $t_z^*$  distributions for an applied dynamic moment  $M_y$  using the Overhauser spline interpolation model. The results were obtained using 16 elements.

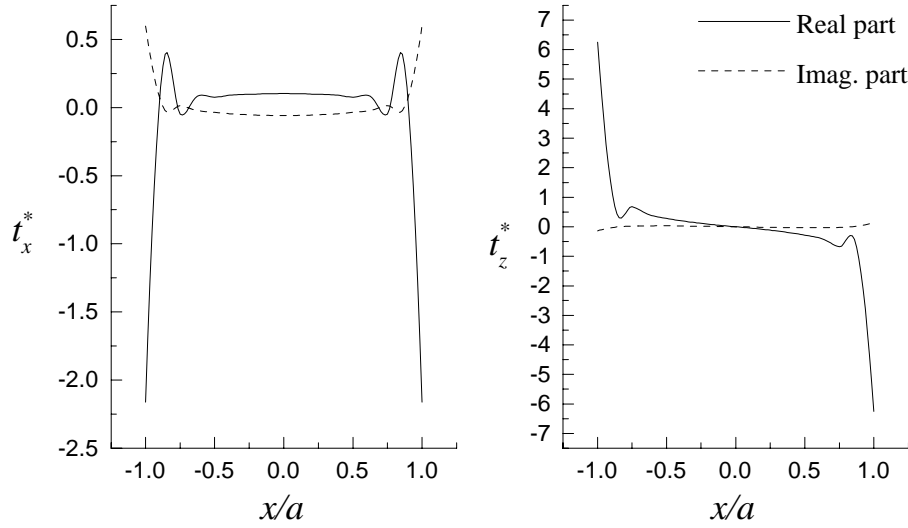


**Figure 8:** Interface traction  $t^*(x)$  distribution due to an applied moment  $M_y$  (Overhauser spline model,  $a_0 = 1$ ,  $\nu = 0.4$ ).

The results show strong oscillations near the foundation edges. Results for the cubic spline interpolation model were also obtained and they are almost equal. As with the linear and quadratic models the singular behavior of the tractions at the foundation edges is clear here. It should be noticed that neither the linear and quadratic models nor the spline models are capable to reproduce correctly this singularity since they all use polynomials.

## 6. SINGULAR INTERPOLATION MODELS

The need of a traction interpolation model that can reproduce well the singular behavior of the interface stresses at the foundation edges is clear from the results presented in the preceding sections. To cope with this singular behavior it is proposed to add special singular segments to the ends of the polynomial interpolation curves. This was done first with the linear interpolation model. The singular function used at the first and last elements are given by (Barros and

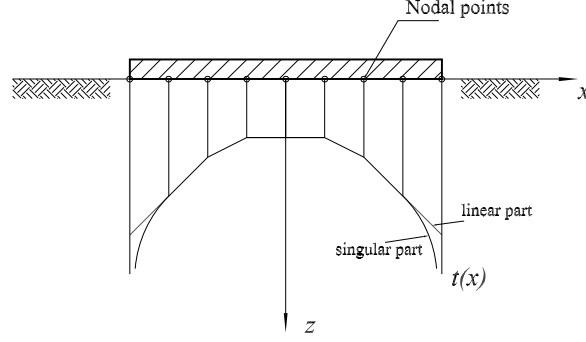


**Figure 9:** Singular-linear interpolation model for the interface tractions  $t_x$  and  $t_z$

Mesquita Neto, 1998):

$$t_j^{(s)}(x) = \frac{1}{\sqrt{1 - \left(\frac{x \pm l}{2l}\right)^2}}, \quad |x| \leq l \quad (13)$$

where the plus sign is used for the first (left) element and the minus sign is used for the last (right) element. This singular function is added to a linear polynomial function obtained by imposing continuity of the  $t'(x)$  at the singular element internal nodes (see Figure 9).

The same singular function is used to create singular-ended spline interpolation models (Barros and Mesquita Neto, 1999). The singular elements are appended to the both ends of the splines and continuity at internal nodes is imposed. For the cubic singular-ended spline  $C^2$  continuity is imposed and for the singular-ended Overhauser spline  $C^1$  continuity is imposed.

The Figures 10 and 11 show the interface traction distributions obtained with the singular-linear and singular-ended Overhauser spline interpolation models respectively. It can be seen that the distributions are much smoother than those obtained with the non singular models. Results for the singular-ended cubic spline model show a similar behavior.

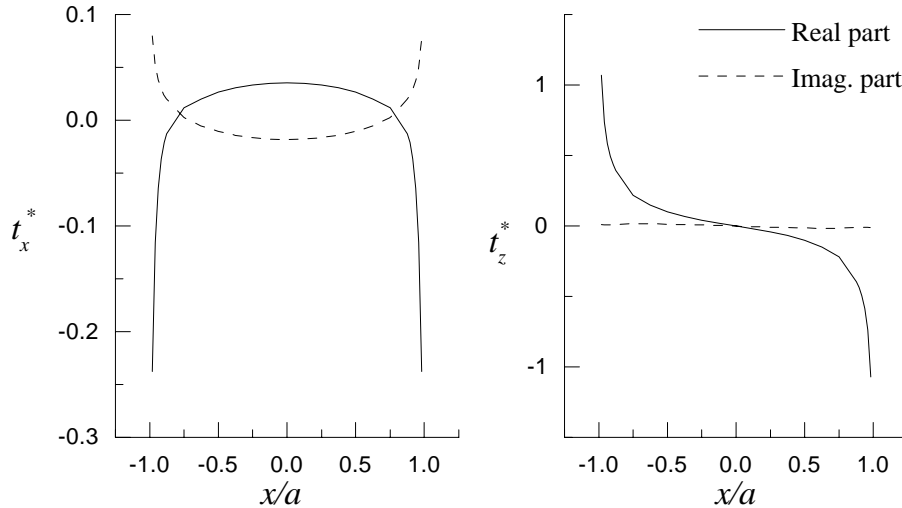


**Figure 10:** Interface traction  $t^*(x)$  distribution due to an applied moment  $M_y$  (singular-linear model,  $a_0 = 1, \nu = 0.4$ ).

The Table 1 shows the number of degrees of freedom  $N^*$  for each one of the interpolation models used here. It also shows the number of influence function evaluations used by these models for both the case of non uniform discretization  $N_1$  and for the case of uniform discretization  $N_2$ .

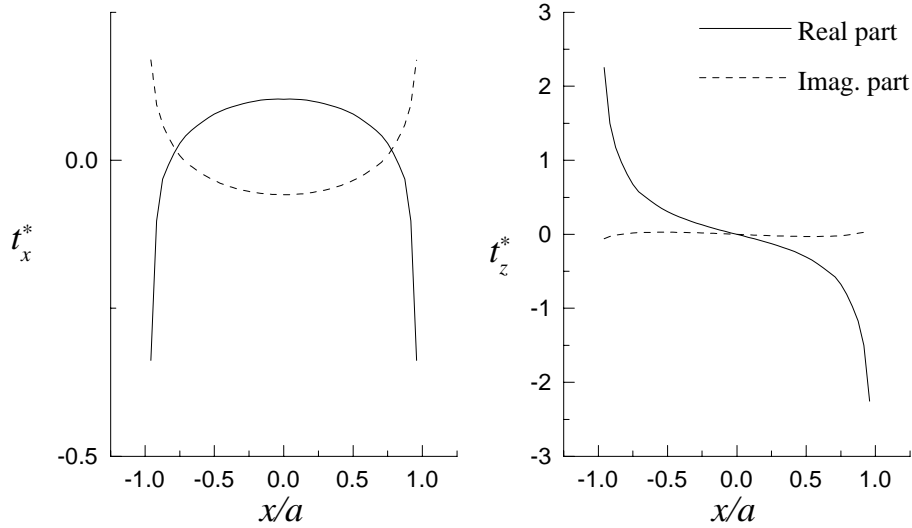


**Figure 11:** Interface traction  $t^*(x)$  distribution due to an applied moment  $M_y$  (singular-ended Overhauser spline model,  $a_0 = 1, \nu = 0.4$ ).

**Table 1:** Number of degrees of freedom and number of influence function evaluation for the interpolation models

Interpolation model	$N^*$	$N_1$	$N_2$
Constant	$N$	$N^2$	$N$
Linear	$N + 1$	$2N^2$	$2N$
Quadratic	$2N + 1$	$6N^2$	$6N$
Splines	$N + 1$	$4N^2$	$4N$
Singular-linear	$N + 1$	$2(N^2 + N + 1)$	$3N + 1$
Singular splines	$N + 1$	$4N^2 - 2N + 6$	$5N - 1$

## 7. ROTATION CONVERGENCE

In order to verify the convergence of the foundation rotation results for the presented traction interpolation models, each one was tested with various (uniform) discretization levels. The plots in Figure 12 show the rotation of a strip foundation bounded to a visco-elastic half-plane ( $\nu = 0.4, v = 0.01$ ) subjected to a dynamic rocking moment  $M_y/a^2 = 1$  with non dimensional frequency  $a_0 = 1$ , as a function of the number of degrees of freedom  $N^*$  of the interpolation model.

The results in Figure 12 show clearly that the interpolation models that incorporate the singular function present better convergence rates. Indeed, it can be seen that these models provide acceptable results even with very small number of elements. On the other hand, the non singular models seems to converge to incorrect values.

## 8. CONCLUDING REMARKS

The various traction interpolation models presented in this work represent a wide survey on the methods that can be used to interpolate the interface stress in the dynamic soil-structure interaction analysis. The results obtained with these various models show that the incorporation of the stresses singular behavior to the interpolation model improves in a great extent the quality of the results and accelerates the convergence. The interpolation methods described herein can be also applied to the analysis of embedded and buried rigid structures. In this case it can be

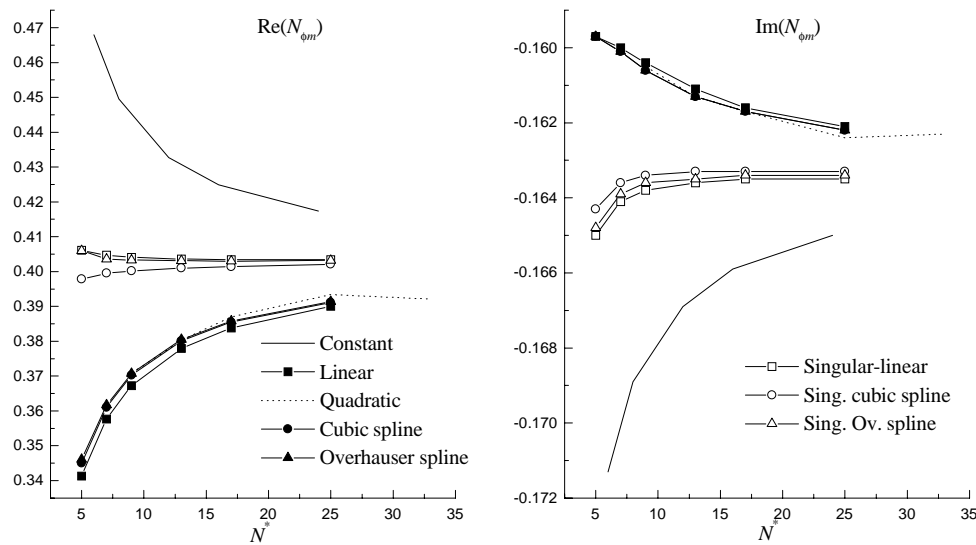


**Figure 12:** Convergence of the rocking compliance  $N_{\phi m}$  with increasing number of degrees of freedom  $N^*$  for various interpolation models.

anticipated that the singular models will also surpass the non singular ones in terms of stresses and displacements determination.

## REFERENCES

- Barros, P. L. A., 1997, *Elastodynamics of Transversely Isotropic Media: Green's Functions and Boundary Element Method Analysis of the Soil-Structure Interaction*, PhD thesis, Faculdade de Engenharia Mecânica, Universidade Estadual de Campinas. In Portuguese.
- Barros, P. L. A. and Mesquita Neto, E., 1998, Singular and higher order elements for accurate interface stresses in dynamic soil-structure interaction, in H. Murakami and J. E. Lucco (eds), *Proceedings of the 12th Engineering Mechanics Conference*, ASCE, pp. 146–149.
- Barros, P. L. A. and Mesquita Neto, E., 1999, Singular-ended spline interpolation for 2D boundary element analysis, *International Journal for Numerical Analysis in Engineering*. In press.
- Brewer, J. A. and Anderson, D. C., 1977, Visual interactions with Overhauser curves and surfaces, *Computer Graphics* **11**, 132–137.
- de Boor, C., 1978, *A Practical Guide to Splines*, Springer-Verlag, New York.
- Lysmer, S., 1965, Vertical motion of rigid footings, Dept. of Civil Engng., University of Michigan, Contract Report No. 3-115. Conducted for WES under Contract No. DA-22-07P-ENG-340.
- Rajapakse, R. N. K. D. and Wang, Y., 1991, Elastodynamic Green's functions of orthotropic half plane, *Journal of Engineering Mechanics* **117**(3), 588–604.